

UNIFIED CONTROL OF MODULAR CASCADED H-BRIDGE MULTILEVEL PV INVERTER CONNECTED TO GRID

A. Sai Ram¹, N. Sammaiah²

¹ Student, EEE Department, Jyothismathi Institute of technology & Science, Telangana, India

² Asst.Prof, EEE Department, Jyothismathi Institute of technology & Science, Telangana, India

ABSTRACT

This paper presents a modular cascaded H-bridge multilevel photovoltaic (PV) inverter for three-phase grid connected applications. The modular cascaded multilevel topology helps to improve the efficiency and flexibility of PV systems. To realize better utilization of PV modules and maximize the solar energy extraction, a distributed maximum power point tracking control scheme is applied to three-phase multilevel inverters, which allows independent control of each dc-link voltage. For three-phase grid-connected applications, PV mismatches may introduce unbalanced supplied power, leading to unbalanced grid current. To solve this issue, a control scheme with modulation compensation is also proposed. Simulation of three-phase seven-level cascaded H-bridge inverter has been built utilizing nine H-bridge modules (three modules per phase). Each H-bridge module is connected to a 185-W solar panel. Simulation results are presented to verify the feasibility of the proposed approach using MATLAB software.

Keyword: - Grid, PV module, Cascaded H-bridge, MPPT

1. INTRODUCTION

In recent days solar energy, has become very popular. Solar-electric-energy demand has grown consistently by 20%–25% per annum over the past 20 years, and the growth is mostly in grid-connected applications. With the extraordinary market growth in grid-connected photovoltaic (PV) systems, there are increasing interests in grid-connected PV configurations.[1]-[4] Traditional methods of power generation, from PV cells, by use of simple inverter circuits, have proven to be vastly ineffective, in view of today's demand for electrical power. Therefore, the introduction of sophisticated inverting methods, like multilevel inverters and cascading of inverters, proved to increase the utilization of solar energy, to supply the increasing demand for electrical power.[5-6] The necessity for balanced power at the generating station cannot be emphasized enough, because the entity of the station is connected to the grid. As such, balanced and in-phase power is to be supplied at load end, so that operation can be continued, as normal.[7]

Cascaded inverters consist of several converters connected in series; thus, the high power and/or high voltage from the combination of the multiple modules would favor this topology in medium and large grid-connected PV systems [8]–[10]. There are two types of cascaded inverters. Fig. 1 shows a cascaded dc/dc converter connection of PV modules [11], [12]. Each PV module has its own dc/dc converter, and the modules with their associated converters are still connected in series to create a high dc voltage, which is provided to a simplified dc/ac inverter. This approach combines aspects of string inverters and ac-module inverters and offers the advantages of individual module maximum power point (MPP) tracking (MPPT), but it is less costly and more efficient than ac-module inverters. However, there are two power conversion stages in this configuration. Another cascaded inverter is shown in Fig. 1 where each PV panel is connected to its own dc/ac inverter, and those inverters are then placed in series to reach a high-voltage level. This cascaded inverter would maintain the benefits of “one converter per panel,” such as better utilization per PV module, capability of mixing different sources, and redundancy of the system. In addition, this dc/ac cascaded inverter removes the need for the per-string dc bus and the central dc/ac inverter, which further improves the overall efficiency.

The modular cascaded H-bridge multilevel inverter, which requires an isolated dc source for each H-bridge, is one dc/ac cascaded inverter topology. The separate dc links in the multilevel inverter make independent voltage control possible. As a result, individual MPPT control in each PV module can be achieved, and the energy harvested from PV panels can be maximized. Meanwhile, the modularity and low cost of multilevel converters would position them as a prime candidate for the next generation of efficient, robust, and reliable grid connected solar power electronics

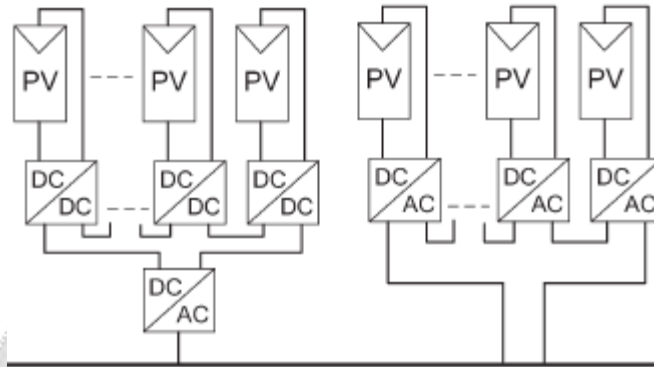


Fig-1: Cascaded DC/DC converter and DC/AC Converter fed to grid

2. PROPOSED CONTROL SCHEME

2.1 Incremental Conductance Method

This method consists in using the slope of the derivative of the current with respect to the voltage in order to reach the maximum power point. The advantage that MPPT gives in the real world depends on the array, their climate, and their seasonal load pattern. It gives us an effective current boost only when the V_{pp} is more than about 1V higher than the battery voltage. In hot weather, this may not be the case unless the batteries are low in charge. In cold weather however, the V_{pp} can rise to 18V. If their energy use is greatest in the winter (typical in most homes) and they have cold winter weather, then they can gain a substantial boost in energy when they need it the most.

Here is an example of MPPT action on a cold winter day: Outside temperature: 20°F (-7°C) Wind is blowing a bit, so the PV cell temperature rises to only around 32°F (0°C). $V_{pp} = 18V$ Batteries are a bit low, and loads are on, so battery voltage = 12.0. Ratio of V_{pp} to battery voltage is $18:12 = 1.5:1$

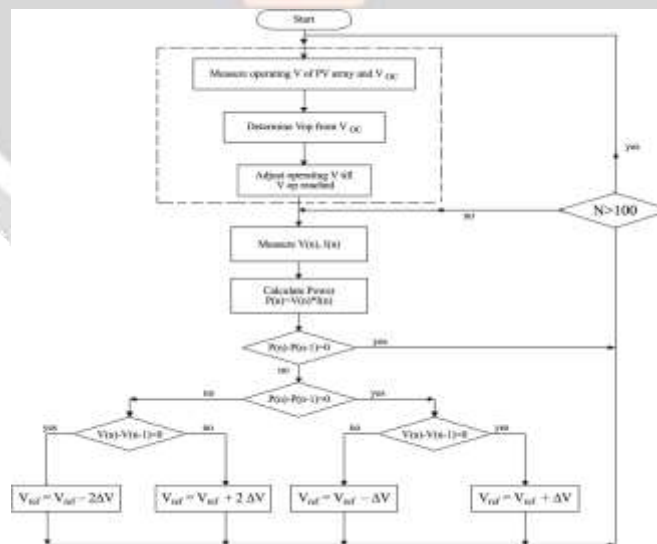


Fig-2: Incremental Conductance Method Algorithm

Under these conditions, a theoretically perfect MPPT (with no voltage drop in the array circuit) would deliver a 50% increase in charge current. In reality, there are losses in the conversion just as there is friction in a car's transmission. Reports from the field indicate that increases of 20 to 30% are typically observed. Both the wind turbine and the photovoltaic array must be adjusted to operate at their point of maximum power. Many different maximum power

point tracking (MPPT) algorithms like perturbation observation method, incremental conductance method have been developed and widely used for such systems. The perturbation observation method is adopted in this paper for both the wind turbine and the photovoltaic array for its simplicity and accuracy. The algorithm starts by choosing an initial reference rotor speed for the wind turbine and an initial reference voltage for the photovoltaic array. The corresponding output powers of the two systems are measured. If this power does not correspond to their maximum powers, then their initial reference values are incremented or decremented by one step. If this adjusts leads to an increase in their output powers then the next adjustment is made in the same direction and vice-versa. The above steps are repeated till the maximum power points of the wind turbine and photovoltaic array are reached.

3 PROPOSED OVERALL SYSTEM

In order to eliminate the adverse effect of the mismatches and increase the efficiency of the PV system, the PV modules need to operate at different voltages to improve the utilization per PV module. The separate dc links in the cascaded H-bridge multilevel inverter make independent voltage control possible. To realize individual MPPT control in each PV module, a control scheme proposed previously is updated for this application.

The distributed MPPT control of the three-phase cascaded H-bridge inverter is shown in Fig. 4.7. In each H-bridge module, an MPPT controller is added to generate the dc-link voltage reference. Each dc-link voltage is compared to the corresponding voltage reference, and the sum of all errors is controlled through a total voltage controller that determines the current reference I_{dref}

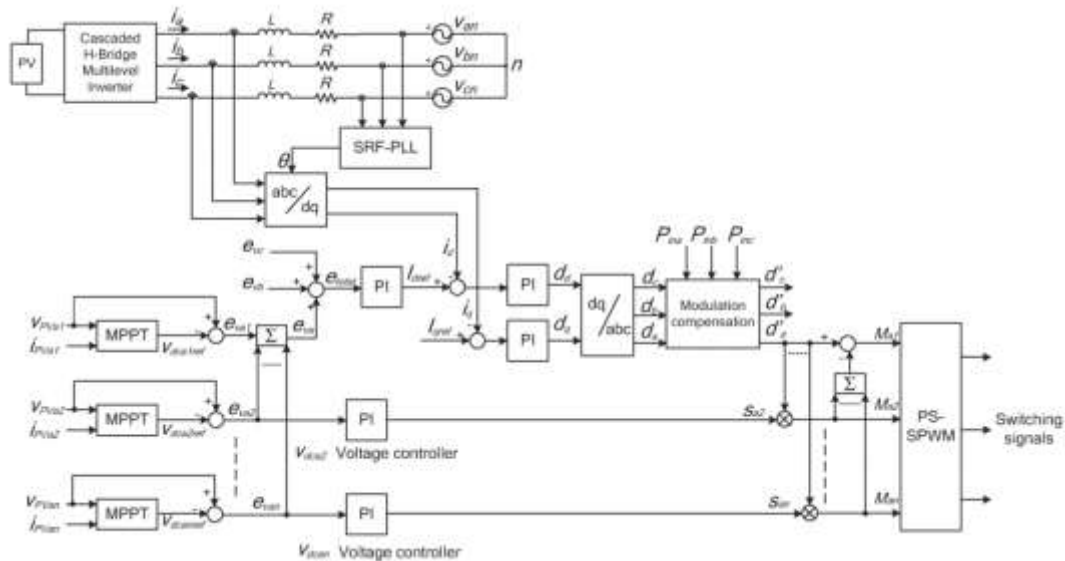


Fig-3: Proposed Control Scheme for three-phase Modular Cascaded H-bridge Multilevel PV inverter

The reactive current reference I_{qref} can be set to zero, or if reactive power compensation is required, I_{qref} can also be given by a reactive current calculator. The synchronous reference frame phase-locked loop (PLL) has been used to find the phase angle of the grid voltage. As the classic control scheme in three-phase systems, the grid currents in abc coordinates are converted to dq coordinates and regulated through proportional-integral (PI) controllers to generate the modulation index in the dq coordinates, which is then converted back to three phases.

The distributed MPPT control scheme for the single-phase system is nearly the same. The total voltage controller gives the magnitude of the active current reference, and a PLL provides the frequency and phase angle of the active current reference. The current loop then gives the modulation index. To make each PV module operate at its own MPP, take phase a as an example; the voltages v_{dca2} to v_{dcan} are controlled individually through $n - 1$ loops. Each voltage controller gives the modulation index proportion of one H-bridge module in phase a. After multiplied by the modulation index of phase a, $n - 1$ modulation indices can be obtained. Also, the modulation index for the first H-bridge can be obtained by subtraction. The control schemes in phases b and c are almost the same. The only difference is that all dc-link voltages are regulated through PI controllers, and n modulation index proportions are obtained for each phase. A phase-shifted sinusoidal pulse width modulation switching scheme is then applied to control the switching devices of each H-bridge. It can be seen that there is one H-bridge module out of N modules whose modulation index is obtained by subtraction. For single-phase systems, $N = n$, and for three-phase systems, N

= 3n, where n is the number of H-bridge modules per phase. The reason is that N voltage loops are necessary to manage different voltage levels on N H-bridges, and one is the total voltage loop, which gives the current reference. So, only N – 1 modulation indices can be determined by the last N – 1 voltage loops, and one modulation index has to be obtained by subtraction.

3.1 MODULATION COMPENSATION SCHEME

As mentioned earlier, a PV mismatch may cause more problems to a three-phase modular cascaded H-bridge multilevel PV inverter. With the individual MPPT control in each H-bridge module, the input solar power of each phase would be different, which introduces unbalanced current to the grid. To solve the issue, a zero sequence voltage can be imposed upon the phase legs in order to affect the current flowing into each phase. If the updated inverter output phase voltage is proportional to the unbalanced power, the current will be balanced.

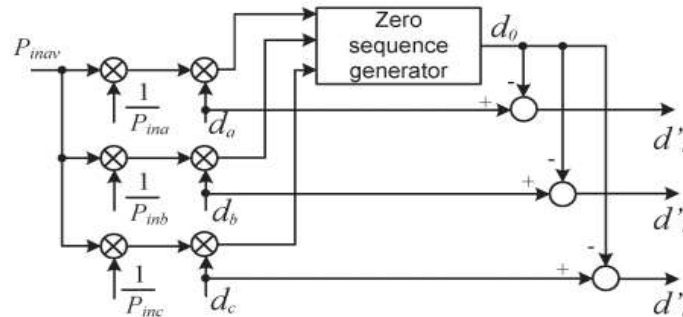


Fig-4: Modulation Compensation Scheme for Proposed Control Scheme

Thus, the modulation compensation block, as shown in Fig. 4.8, is added to the control system of three-phase modular cascaded multilevel PV inverters. The key is how to update the modulation index of each phase without increasing the complexity of the control system. First, the unbalanced power is weighted by ratio r_j , which is calculated as

$$r_j = \frac{P_{inav}}{P_{inj}}$$

where P_{inj} is the input power of phase j ($j = a, b, c$), and P_{inav} is the average input power.

Then, the injected zero sequence modulation index can be generated as

$$d_0 = \frac{1}{2} [\min(r_a \cdot d_a, r_b \cdot d_b, r_c \cdot d_c) + \max(r_a \cdot d_a, r_b \cdot d_b, r_c \cdot d_c)]$$

where d_j is the modulation index of phase j ($j = a, b, c$) and is determined by the current loop controller.

The modulation index of each phase is updated by

$$d'_j = d_j - d_0$$

Only simple calculations are needed in the scheme, which will not increase the complexity of the control system. An example is presented to show the modulation compensation scheme more clearly. Assume that the input power of each phase is unequal

$$P_{ina} = 0.8 \quad P_{inb} = 1 \quad P_{inc} = 1.$$

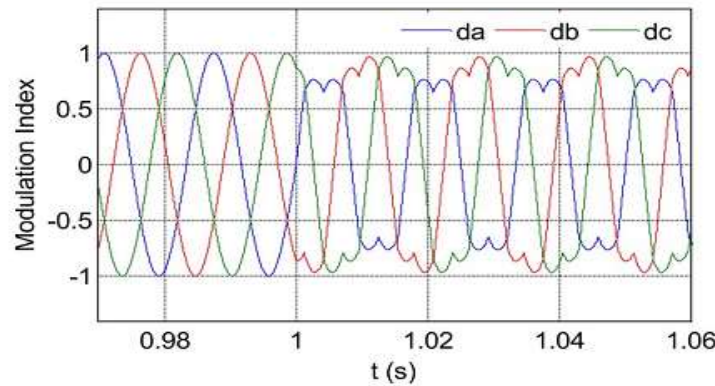


Fig-5: Modulation Indices before and after Modulation Compensation

By injecting a zero sequence modulation index at $t = 1$ s, the balanced modulation index will be updated, as shown in Fig. 4.9. It can be seen that, with the compensation, the updated modulation index is unbalanced proportional to the power, which means that the output voltage (v_{jN}) of the three-phase inverter is unbalanced, but this produces the desired balanced grid current.

3.2 Active and Reactive Power Measurement in Three Phase System

The reactive power recognized as an essential factor in the conception and the efficient operating of AC electric network. The application of Clark (α - β) and Park (d-q) transforms to three phase system in order to calculate the instantaneous active and reactive power is a useful tool for study and analysis of many electrical systems. There are many industrial applications that require the knowledge of the instantaneous value of the active and reactive power. In fact, they are used to manage the economical aspect of their system. The instantaneous active and reactive powers are also used in the control of converters connected to electric network. These converters can control the flow of active and reactive power in the power system to improve voltage regulation, and increasing transient stability margin.

3.2.1 Theoretical Analysis of Clark (α - β) & Park (d-q) Coordinates transformation

Voltages and currents can be transformed from abc system to α - β coordinates as follows, where X denotes voltage or current:

$$\begin{bmatrix} X_\alpha \\ X_\beta \\ X_0 \end{bmatrix} = \sqrt{\frac{2}{3}} \begin{bmatrix} 1 & -\frac{1}{2} & -\frac{1}{2} \\ 0 & \frac{\sqrt{3}}{2} & -\frac{\sqrt{3}}{2} \\ \frac{1}{\sqrt{2}} & \frac{1}{\sqrt{2}} & \frac{1}{\sqrt{2}} \end{bmatrix} \begin{bmatrix} X_a \\ X_b \\ X_c \end{bmatrix}$$

From α - β transformation the d-q coordinates are given by:

$$\begin{bmatrix} X_d \\ X_q \\ X_o \end{bmatrix} = \begin{bmatrix} \cos(\omega t) & \sin(\omega t) & 0 \\ -\sin(\omega t) & \cos(\omega t) & 0 \\ 0 & 0 & 1 \end{bmatrix} \begin{bmatrix} X_\alpha \\ X_\beta \\ X_o \end{bmatrix}$$

The active and reactive power for three phase balanced system can be written in d-q coordinates as follows, where V_d , V_q , I_d and I_q care the voltages and currents in d-q coordinates.

$$P = V_d I_d + V_q I_q$$

$$Q = V_d I_q - V_q I_d$$

4 SIMULATION RESULTS

The preregulator operation with nominal output power and input voltage equal to $V_i = 127 V_{rms}$ are presented from Figs. 23 to 30, considering the operation with the third-harmonic reduction technique. The $L1$ and $L2$ currents are presented in Fig. 23

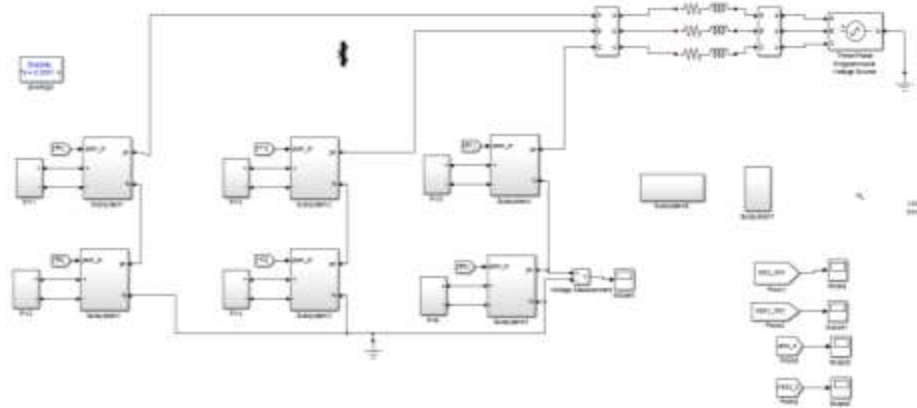


Fig-6: Simulation of proposed system using MATLAB

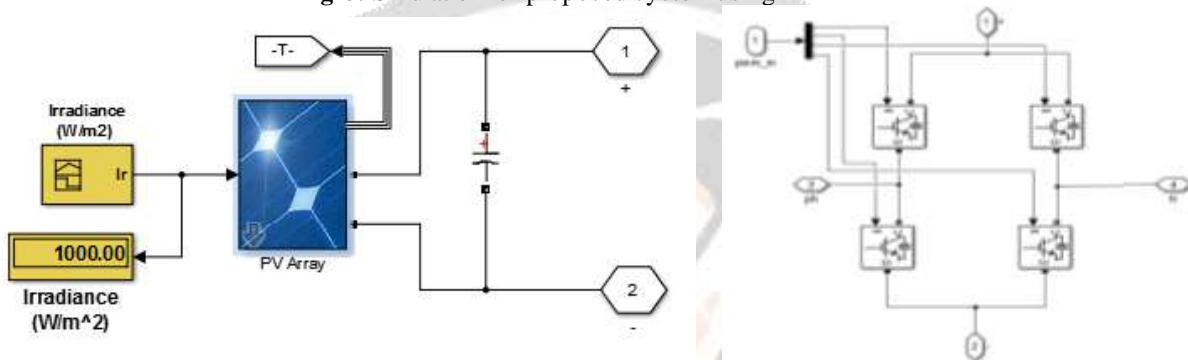


Fig-7: Solar PV module and H-Bridge Inverter

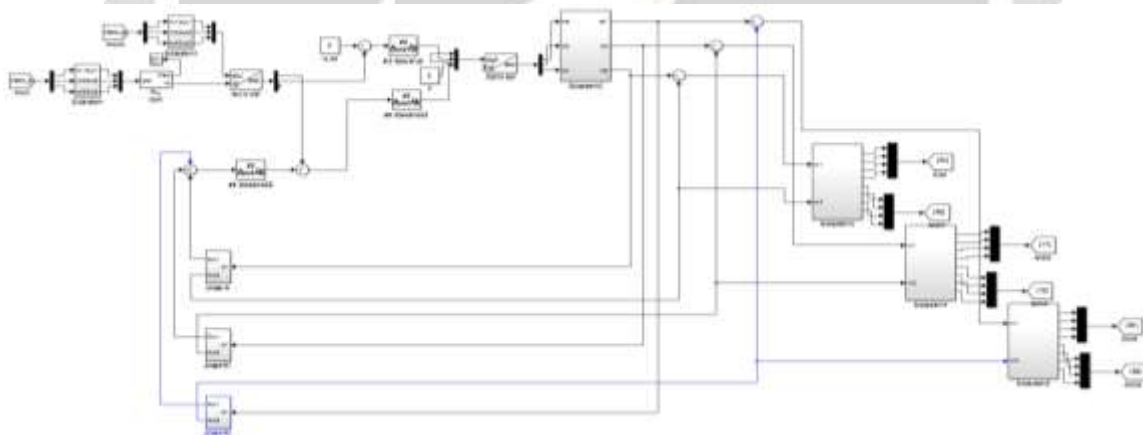


Fig-8: Proposed control strategy

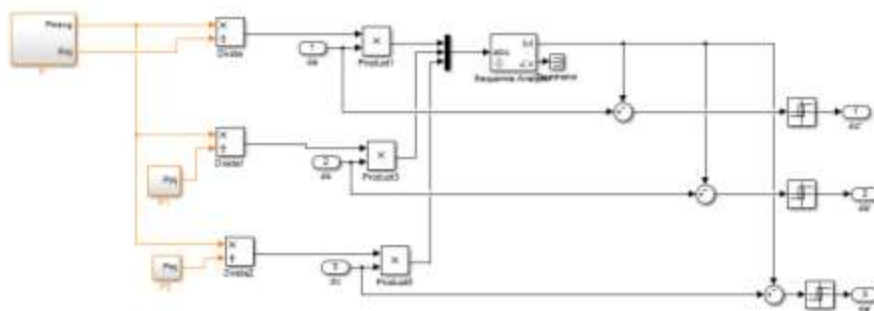


Fig-9: Modulation Indices before and after Modulation Compensation

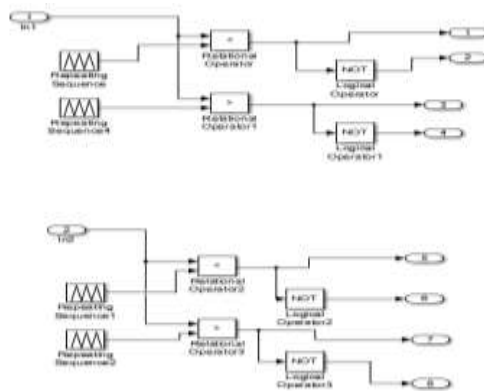


Fig-10: PWM scheme applied to proposed controller

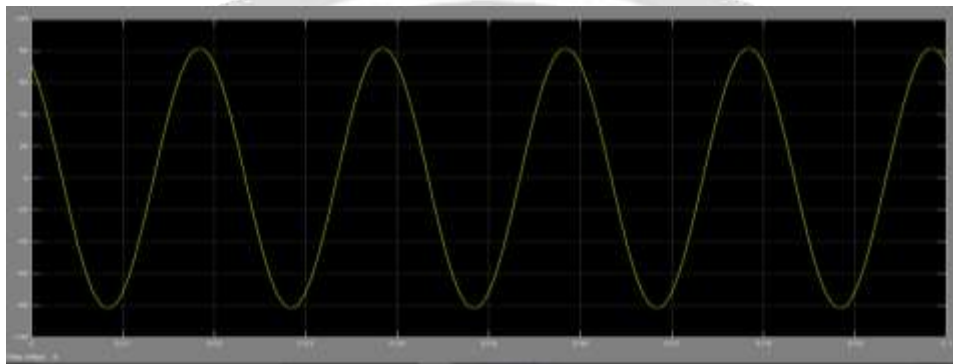


Fig-11: Output voltage waveform of individual CHB

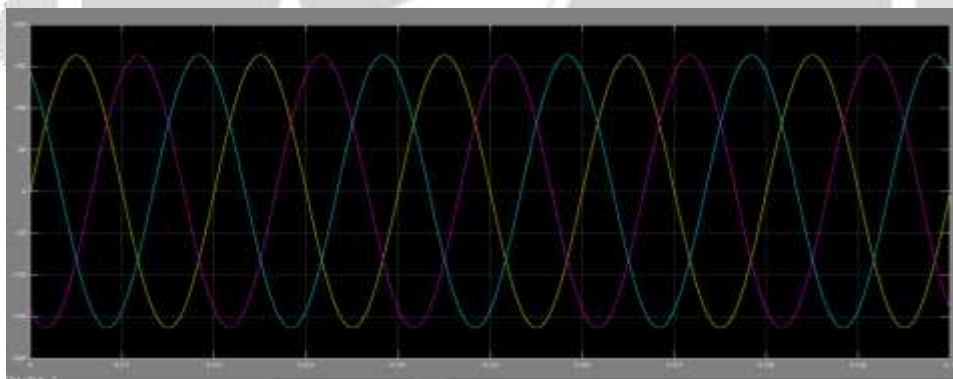


Fig-12: Overall system current waveform

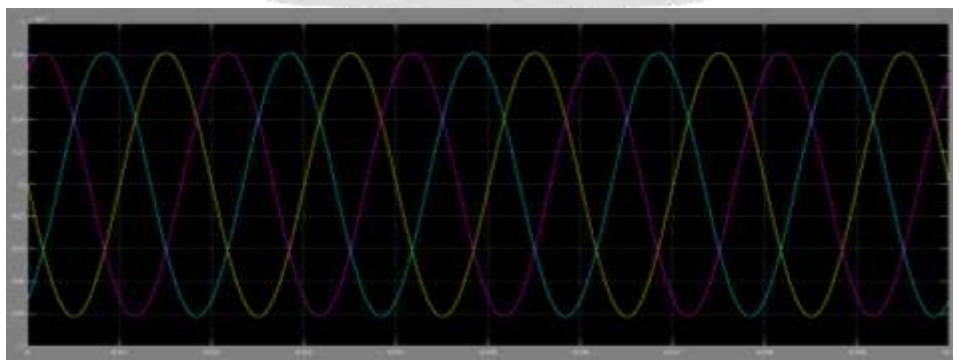


Fig-13: Grid injected currents and voltages

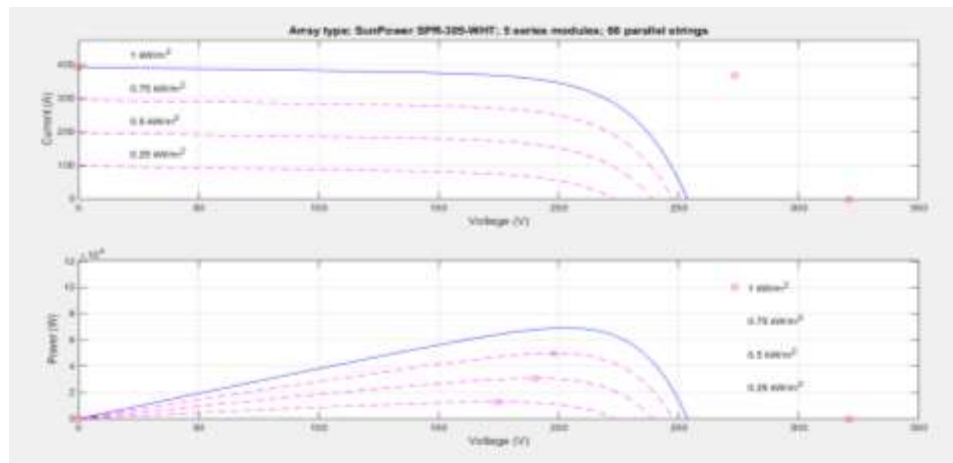


Fig-14: power factor when using Fuzzy logic controller

5. CONCLUSIONS

In this paper, a modular cascaded H-bridge multilevel inverter for grid-connected PV applications has been presented. The multilevel inverter topology will help to improve the utilization of connected PV modules if the voltages of the separate dc links are controlled independently. Thus, a distributed MPPT control scheme for both single- and three-phase PV systems has been applied to increase the overall efficiency of PV systems. For the three-phase grid-connected PV system, PV mismatches may introduce unbalanced supplied power, resulting in unbalanced injected grid current. A modulation compensation scheme, which will not increase the complexity of the control system or cause extra power loss, is added to balance the grid current. In the upcoming years, the proposed project is expected to be implemented in PV generation units, in developed countries utilizing PV energy as their primary power source. In such a case scenario, the potential increment in overall efficiency, as well as the substantial decrease in long-term investment capital is quite formidable to introspect. That said, it is not definite that this development will remain as the best option, for PV inverters; given that developments are being made every day to improve on previous designs. Thus, before implementation of the proposed scheme, care should be taken to include potential future improvements to the design.

6. REFERENCES

- [1] O. Garc'ia, J. A. Cobos, R. Prieto, P. Alou, and J. Uceda, "Single phase power factor correction: A survey," *IEEE Trans. Power Electron.*, vol. 18, no. 3, pp. 749–755, May 2003.
- [2] M.M. Jovanovic and Y. Jang, "State-of-the-art, single-phase, active power factor-correction techniques for high-power applications—An overview," *IEEE Trans. Ind. Electron.*, vol. 52, no. 3, pp. 701–708, Jun. 2005.
- [3] D. S. L. Simonetti, J. Sebastian, and J. Uceda, "The discontinuous conduction mode SEPIC and CUK power factor pre regulators: Analysis and design," *IEEE Trans. Ind. Electron.*, vol. 44, no. 5, pp. 630–637, Oct. 1997.
- [4] M. Mahdavi and H. Farzanehfar, "Bridgeless SEPIC PFC rectifier with reduced components and conduction losses," *IEEE Trans. Ind. Electron.*, vol. 58, no. 9, pp. 4153–4160, Sep. 2011.
- [5] A. A. Fardoun, E. H. Ismail, A. J. Sabzali, and M. A. Al-Saffar, "New efficient bridgeless Cuk rectifiers for PFC applications," *IEEE Trans. Power Electron.*, vol. 27, no. 7, pp. 3292–3301, Jul. 2012.
- [6] E. H. Ismail, "Bridgeless SEPIC rectifier with unity power factor and reduced conduction losses," *IEEE Trans. Ind. Electron.*, vol. 56, no. 4, pp. 1147–1157, Apr. 2009.
- [7] B. Su, J. Zhang, and Z. Lu, "Totem-pole boost bridgeless pfc rectifier with simple zero-current detection and full-range zvs operating at the boundary of DCM/CCM," *IEEE Trans. Power Electron.*, vol. 26, no. 2, pp. 427–435, Feb. 2011.
- [8] J. Zhang, B. Su, and Z. Lu, "Single inductor three-level bridgeless boost power factor correction rectifier with nature voltage clamp," *IET Power Electron.*, vol. 5, no. 3, pp. 358–365, Mar. 2012.
- [9] Y. Cho and J.-S. Lai, "Digital plug-in repetitive controller for single-phase bridgeless pfc converters," *IEEE Trans. Power Electron.*, vol. 28, no. 1, pp. 165–175, Jan. 2013.
- [10] A. A. Fardoun, E. H. Ismail, A. J. Sabzali, and M. A. Al-Saffar, "Bridgeless resonant pseudo boost PFC rectifier," *IEEE Trans. Power Electron.*, vol. 29, no. 11, pp. 5949–5960, Nov. 2014.

- [11] R. Gules, W. M. Santos, F. A. Reis, E. F. R. Romaneli, and A. A. Badin, "A modified SEPIC converter with high static gain for renewable applications," *IEEE Trans. Power Electron.*, vol. 29, no. 11, pp. 5860–5871, Nov. 2014.
- [12] P. F. de Melo, R. Gules, E. F. R. Romaneli, and R. C. Annunziato, "A modified SEPIC converter for high-power-factor rectifier and universal input voltage applications," *IEEE Trans. Power Electron.*, vol. 25, no. 2, pp. 310–321, Feb. 2010.

